AD-A187 982 DEVELOPMENT AND APPLICATION OF OXYGEN FLOW TAGGING FOR VELOCITY MEASUREME (U) PRINCETON UNIV NJ DEPT OF MECHANICAL AND AEROSPACE ENGINEERIN R B MILES

1/1

UNCLASSIFIED 10 SEP 87 AFOSR-TR-87-1707 AFOSR-86-0191 F/G 14/2 NL

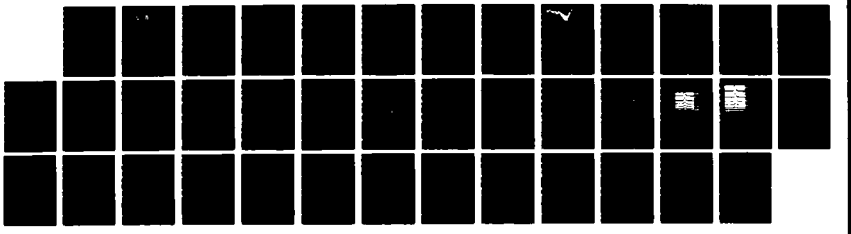

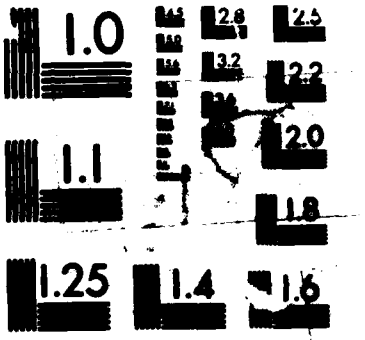

MICROCOPY RESOLUTION TEST CHART
NS-1963-A

UNCLASSIFIED AFOSR FILE COPY

(2)

AD-A187 982

TIC ELECTE NOV 3 0 1987 S D

REPORT DOCUMENTATION PAGE

1b RESTRICTIVE MARKINGS

2a SECURITY CLASSIFICATION AUTHORITY

3 DISTRIBUTION/AVAILABILITY OF REPORT

APPROVED FOR PUBLIC RELEASE
DISTRIBUTION IS UNLIMITED

2b DECLASSIFICATION/DOWNGRADING SCHEDULE

4 PERFORMING ORGANIZATION REPORT NUMBER(S)

5 MONITORING ORGANIZATION REPORT NUMBER(S)

AFOSR-TR- 87-1707

6a NAME OF PERFORMING ORGANIZATION
Prof. Richard B. Miles
Princeton University, MAE Dept.

6b OFFICE SYMBOL (If applicable)

7a NAME OF MONITORING ORGANIZATION
AFOSR/NA

6c ADDRESS (City, State and ZIP Code)
Princeton University, MAE Dept.
D-414 Engineering Quad., Olden St.
Princeton, NJ 08544

7b ADDRESS (City, State and ZIP Code)
BUILDING 410
BOLLING AFB, DC 20332-6448

8a NAME OF FUNDING/SPONSORING ORGANIZATION
AFOSR/NA

8b OFFICE SYMBOL (If applicable)
NA

9 PROCUREMENT INSTRUMENT IDENTIFICATION NUMBER
AFOSR-86-0191

8c ADDRESS (City, State and ZIP Code)
BUILDING 410
BOLLING AFB, DC 20332-6448

10 SOURCE OF FUNDING NOS

PROGRAM ELEMENT NO	PROJECT NO.	TASK NO.	WORK UNIT NO.
61102F	2307	A2	

11. TITLE (Include Security Classification) Development & Application
(U) Oxygen Flow Tagging for Velocity Measurements
& Flow Visualization in Turbulent 3-D Supersonic Flows

12. PERSONAL AUTHOR(S)
Miles, Richard B.

13a TYPE OF REPORT	13b TIME COVERED	14 DATE OF REPORT (Yr., Mo., Day)	15. PAGE COUNT
Annual Tech. Report	FROM 6/1/86 TO 5/31/87	September 10, 1987	37

16. SUPPLEMENTARY NOTATION

17 COSATI CODES		
FIELD	GROUP	SUB GR

18 SUBJECT TERMS (Continue on reverse if necessary and identify by block number)
Flow Diagnostics; Velocity Measurements; Temperature Measurements; Density Measurements; Laser Diagnostics; Supersonic Flows; Turbulent + three dimensional flows

19. ABSTRACT (Continue on reverse if necessary and identify by block number)

During this first year of research work has concentrated on the acquisition of laser systems and the contruction of our test facility. ~~In addition,~~ we have achieved two major research milestones: the demonstration of velocity tagging, and the demonstration of the simultaneous measurement of two-dimensional temperature and pressure fields. We are currently studying the nonlinear effects associated with high intensity laser fields with a particular interest in how they affect the measurements of flow properties.

20 DISTRIBUTION/AVAILABILITY OF ABSTRACT

UNCLASSIFIED/UNLIMITED ☒ SAME AS RPT ☐ DTIC USERS ☐

21 ABSTRACT SECURITY CLASSIFICATION

UNCLASSIFIED

22a NAME OF RESPONSIBLE INDIVIDUAL	22b TELEPHONE NUMBER (Include Area Code)	22c OFFICE SYMBOL
JAMES M MCMICHAEL	202-767-4935	AFOSR/NA

DD FORM 1473, 83 APR EDITION OF 1 JAN 73 IS OBSOLETE.

UNCLASSIFIED

SECURITY CLASSIFICATION OF THIS PAGE

A

Annual Technical Report for AFOSR-86-0191

DEVELOPMENT AND APPLICATION OF OXYGEN FLOW TAGGING FOR VELOCITY MEASUREMENTS AND FLOW VISUALIZATION IN TURBULENT THREE-DIMENSIONAL SUPERSONIC FLOWS

Richard B. Miles
MECHANICAL & AEROSPACE ENGINEERING
PRINCETON UNIVERSITY
Princeton, NJ 08544

September 10, 1987

During this first year of research, work has concentrated on the acquisition of laser systems and the construction of our test facility. In addition, we have achieved two major research milestones: the demonstration of velocity tagging, and the demonstration of the simultaneous measurement of two-dimensional temperature and pressure fields. We are currently studying the nonlinear effects associated with high intensity laser fields with a particular interest in how they effect the measurements of flow properties.

A. LABORATORY CONSTRUCTION AND LASER ACQUISITION

The major construction activity has been the building of a supersonic axisymmetric test facility with its associated high pressure gas handling capabilities. A diagram of the gas flow facility is shown in Fig. 1. The major funding for this facility has come from a DoD-URIP Grant, together with approximately $80,000 for support from Princeton University. The vertical wind tunnel is designed to operate up to Mach 3 with a 1/2-inch diameter nozzle. We expect, however, that most experiments will be done with a 1/4-inch diameter nozzle to maximize run time and minimize noise. A contoured 1/4-inch Mach 1 orifice has been machined and will be used for preliminary measurements. At present, the wind tunnel has been completed with the exception of the installation of the quartz windows. The entire system has been test run and is operational. No experiments using the wind tunnel facility have yet been undertaken.

A state-of-the-art Nd:YAG laser has been installed, which is capable of producing very high energy (1 Joule) with an exceptionally narrow linewidth. This laser is the first of its kind to be delivered by Quantel and gives us the ability to efficiently excite specific rotational transitions of the oxygen molecule. As a consequence, the laser system can be optimized for the temperature of the oxygen so that a maximum number of oxygen molecules can be driven into the vibrationally excited state.

We have also installed a state-of-the-art injection narrowed argon-fluoride laser which permits us to efficiently interrogate these molecules by tuning that laser to a specific electronic transition for maximum fluorescence. This was also one of the first of its kind to be delivered, and, in both cases, we have been working together with the manufacturer to achieve consistent performance.

Additional construction projects have included the building of a test cell in which our initial proof-of-concepts experiments have been done, the construction of a heated oxygen/air jet facility which has allowed us to develop the temperature and density measurement method, and the installation of data acquisition systems, spectrometers, gas purging apparatus, etc.

B. RESEARCH RESULTS

The major research accomplishments from this work are summarized in the attached preprints (Appendices I and II). We have demonstrated that oxygen molecules may be tagged and followed in both oxygen and air flows, allowing one to quantitatively determine three-dimensional velocity profiles and flow structures. We have also developed a new method for instantaneous two-dimensional temperature and density measurements in oxygen or air. With the present laser and detector set-up, the temperature cannot be accurately determined below about 500 K. By switching to ultraviolet detectors and using a Raman-shifted laser, low temperature fields are expected to be observable.

With respect to the time-line (Fig. 2), the following progress has been made: (Note: actual funding began 6/1/86, not 4/1/86 as shown on the figure.)

1. Proof-of-concept velocity measurement experiments have been completed in a static cell and are reported in Appendix I. The experiment is now being configured so that continuing tests with the static cell can be run in parallel with the wind tunnel tests.

2. Work on the narrow linewidth single-mode dye laser has been temporarily discontinued since the new Nd:YAG laser/dye laser has sufficiently narrow linewidth to selectively excite specific rotational states. An example of the difference between a standard Nd:Yag laser/dye laser and a narrow linewidth version is shown in Fig. 3. Both curves represent the rotational structure of the Q branch which is used to pump the oxygen into the first vibrational state. The upper curve was done with a standard Nd:YAG laser/dye laser, and the lower curve was done with the new frequency narrowed version. Note in the lower curve that the individual rotational lines are well resolved. We are also using this laser to study the effects of very high power on the pumping mechanism, as shown in Fig. 4. Here again, the upper curve is with the older version of the laser system, and the lower curve is with the new frequency narrowed version. Individual lines have been distorted by

saturation and Stark broadening processes associated with high laser intensity.

3. The Raman shifter has been built and tested with both hydrogen and deuterium. The center of the Raman shifter is surrounded with a vacuum-insulated liquid nitrogen reservoir to yield significant enhancement of the Raman shifting efficiency. Since we have observed good fluorescence intensity in the oxygen flow tagging experiment without the Raman shifter, it has not yet been incorporated into the system. It will, however, be necessary for measuring low temperature fields and will be integrated into the system when those experiments are undertaken.

4. Much of the work on temperature and density measurements has involved determining the characteristics of the argon-fluoride laser system and the absorption/fluorescence of oxygen which has been excited by that laser. Continued observation of fluorescence, particularly in the presence of very high intensity tagging lasers, is currently underway.

5. The axisymmetric wind tunnel facility should be operational in the near future. As previously mentioned, the compressor, flow control system, high pressure plumbing, and exhaust system have all been separately tested and run satisfactorily. As soon as the windows have been properly mounted, tests for this system will be started.

6. Proof-of-concept experiments for multiple point pressure and temperature measurements are currently underway. Preliminary results are discussed in Appendix II. Support for this work has been shared with Lockheed California Corporation.

C. PUBLICACTIONS AND REPORTS

1. "Multi-Point Oxygen Flow Tagging by Raman Excitation + Laser Induced Electronic Fluorescence," R. Miles, November 24-26, 1985, Thirty-Eighth Meeting of the Division of Fluid Dynamics, American Physical Society, Bulletin of the American Physical Society 30, Paper CH-3, page 1720, New York: American Physical Society, 1985.

2. "Oxygen Flow Tagging by Raman Excitation Plus Laser-Induced Electronic Fluorescence," R. Miles, June 1986, CLEO'86/IQEC'86, Conference on Lasers and Electro-Optics, San Francisco, California (Invited Paper).

3. "Time Resolved Velocity Profiles by Vibrational Tagging of Oxygen," R. Miles, J. Connors, S. Huang, E. Markovitz, and G. Russell, April 1987, CLEO'87/IQEC'87, Conference on Lasers and Electro-Optics, Baltimore, Maryland (Post Deadline Paper).

4. "Velocity Measurements by Vibrational Tagging and Fluorescent Probing of Oxygen," R. Miles, C. Cohen, J. Connors, P. Howard, S. Huang, E. Markovitz, and G. Russell, Optics Letters (To be published November 1987).

5. "Single-Pulse Temperature and Density Cross Sections of Oxygen and Air," R. Miles, J. Connors, P. Howard, E. Markovitz, and G. Roth, (Submitted for publication).

6. "Instantaneous 2D Temperature and Density Measurements in Oxygen and Air," R. Miles, J. Connors, E. Markovitz, G. Roth, and P. Howard, 40th Anniversary Meeting of the Division of Fluid Dynamics of the American Physical Society, Eugene, Oregon, November 22-24, 1987 (Submitted Paper).

7. "Coherent Anti-Stokes Raman Scattering (CARS) and Raman Pumping Line Shapes in High Fields," R. Miles, J. Connors, E. Markovitz, and P. Howard, SPIE's O-E/LASE'88 Third Annual Technical Symposium on Optoelectronics and Laser Applications in Science and Engineering, Los Angeles, California, January 10-15, 1988 (Invited Paper).

D. PERSONNEL

Two new graduate students, Ed Markovitz and John Connors, joined our research group in the summer of 1986 and have been working on this experiment. In addition, Gregory Russell has been working as a research assistant concentrating on the data and image processing aspects of the work. Phil Howard was hired in December 1986 as a technician to oversee the completion of the laboratory construction and to be responsible for the operation of the wind tunnel and laser facilities. Major contributions have been made by undergraduate students, including Chris Moore, who designed the test cell and the wind tunnel; Peter Lasky, who designed the Raman shifter; Clark Cohen, who built the narrow linewidth single-mode dye laser and did preliminary tests on coherent anti-Stokes Raman scattering and argon-fluoride laser-induced fluorescence; and Greg Roth, who has done computer modelling of the oxygen Rayleigh scattering and fluorescence signals.

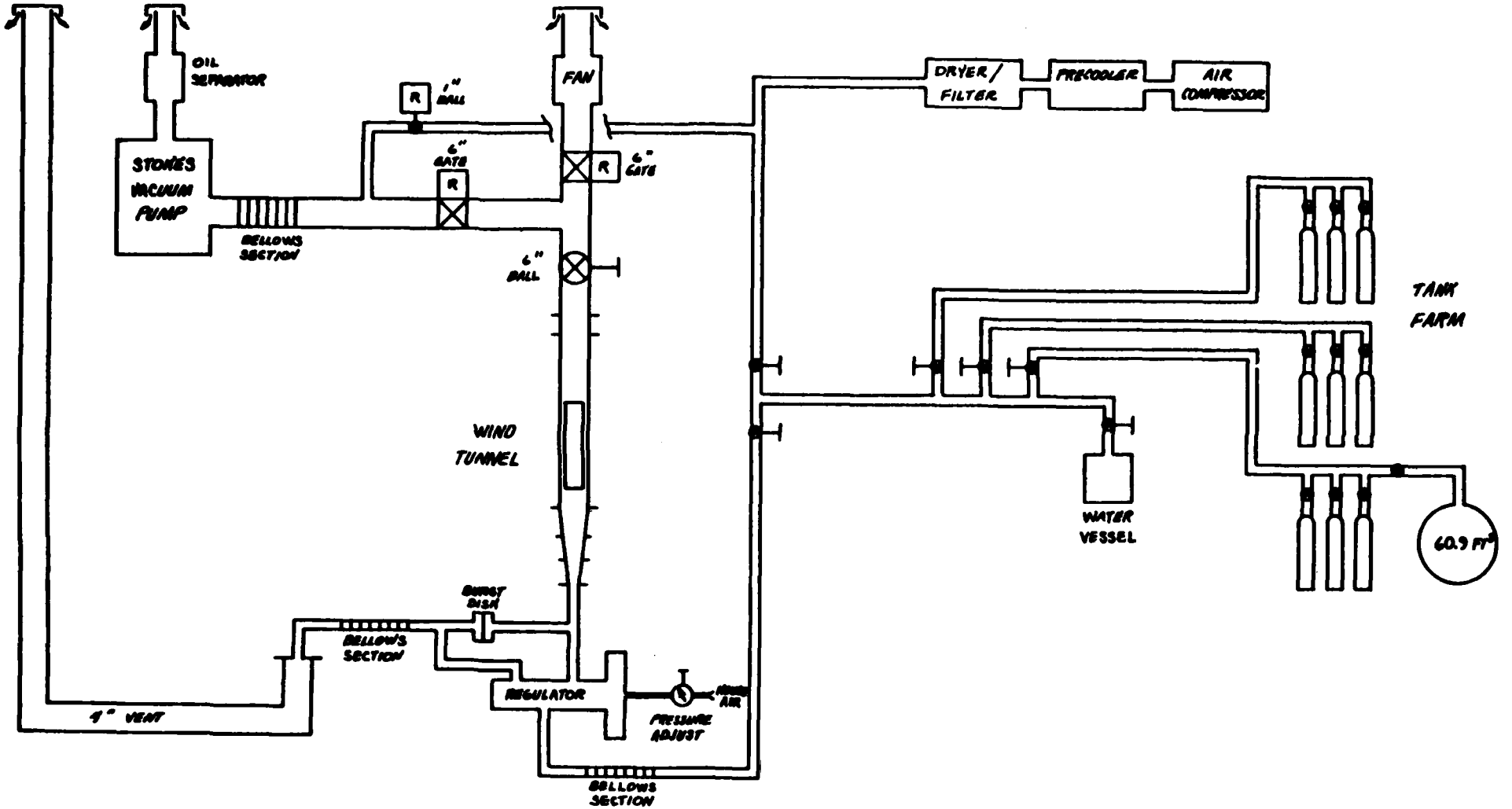

FIGURE 1

DIAGRAM OF THE GAS FLOW FACILITIES

FIGURE 2

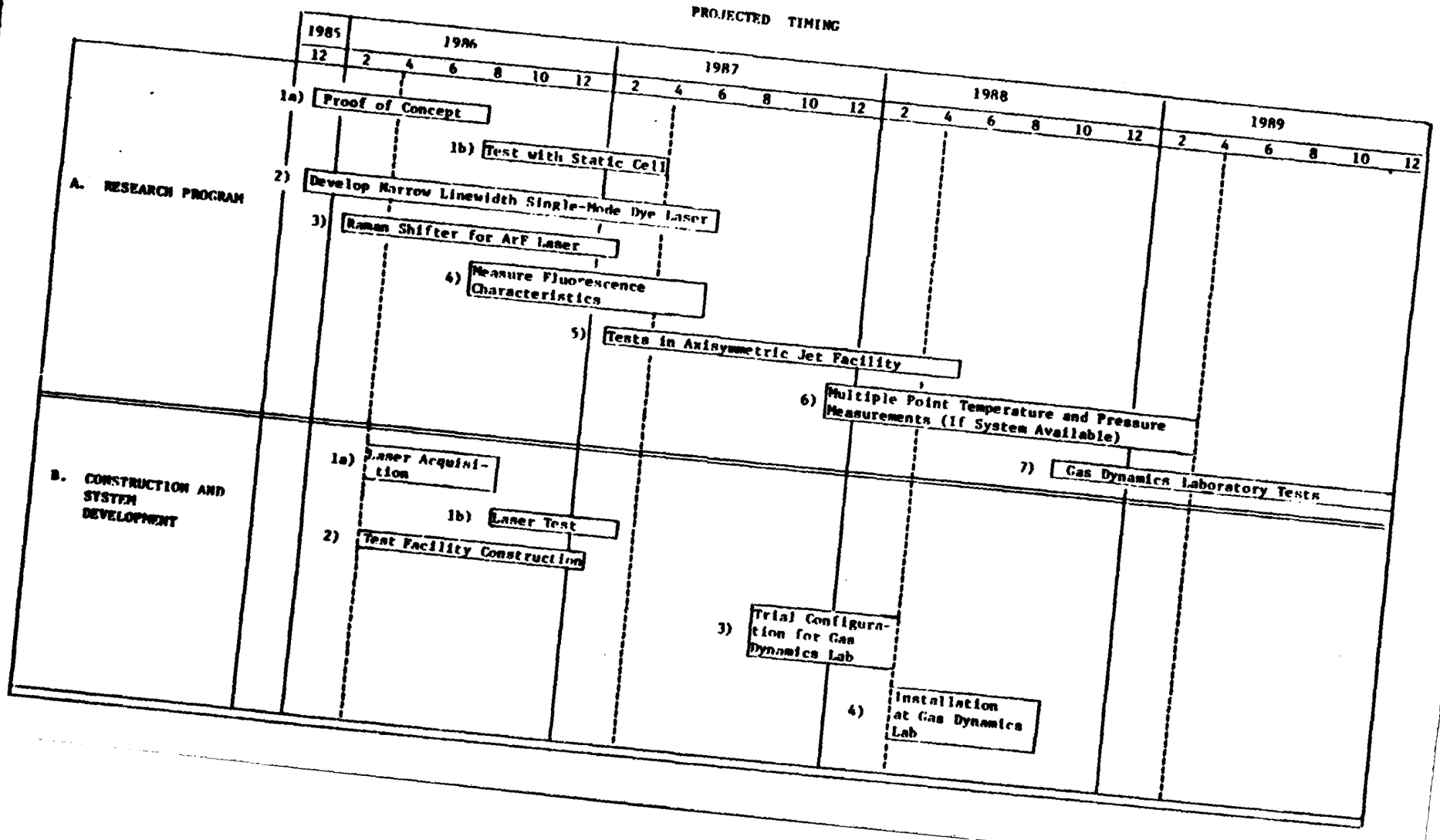
PROJECTED TIMING
1985
1986
1987
1988
1989
12 2 4 6 8 10 12 2 4 6 8 10 12 2 4 6 8 10 12 2 4 6 8 10 12
A. RESEARCH PROGRAM
1a) Proof of Concept
1b) Test with Static Cell
2) Develop Narrow Linewidth Single-Mode Dye Laser
3) Raman Shifter for ArF Laser
4) Measure Fluorescence Characteristics
5) Tests in Axisymmetric Jet Facility
6) Multiple Point Temperature and Pressure Measurements (If System Available)
7) Gas Dynamics Laboratory Tests
B. CONSTRUCTION AND SYSTEM DEVELOPMENT
1a) Laser Acquisition
1b) Laser Test
2) Test Facility Construction
3) Trial Configuration for Gas Dynamics Lab
4) Installation at Gas Dynamics Lab

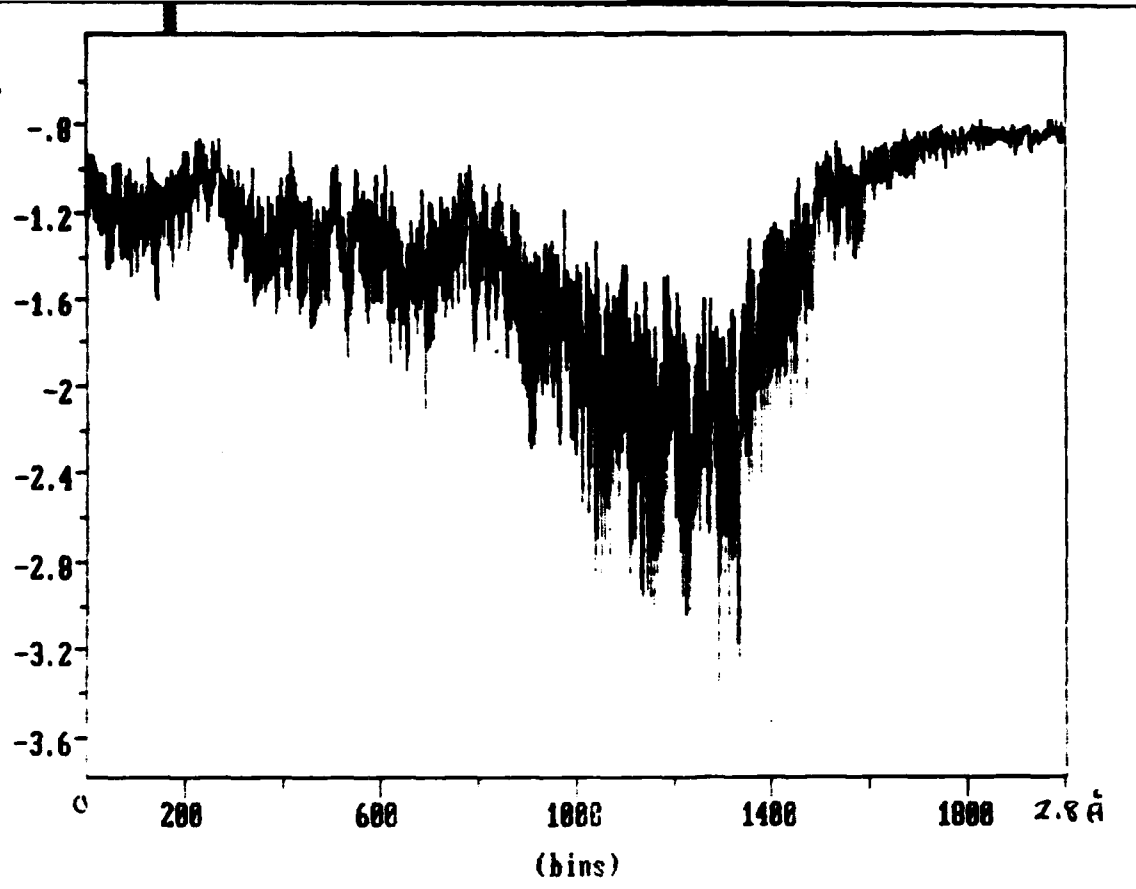
Low Power
-.8
-1.2
-1.6
-2
-2.4
-2.8
-3.2
-3.6
0
200
600
1000
1400
1800
2.8 Å
(bins)

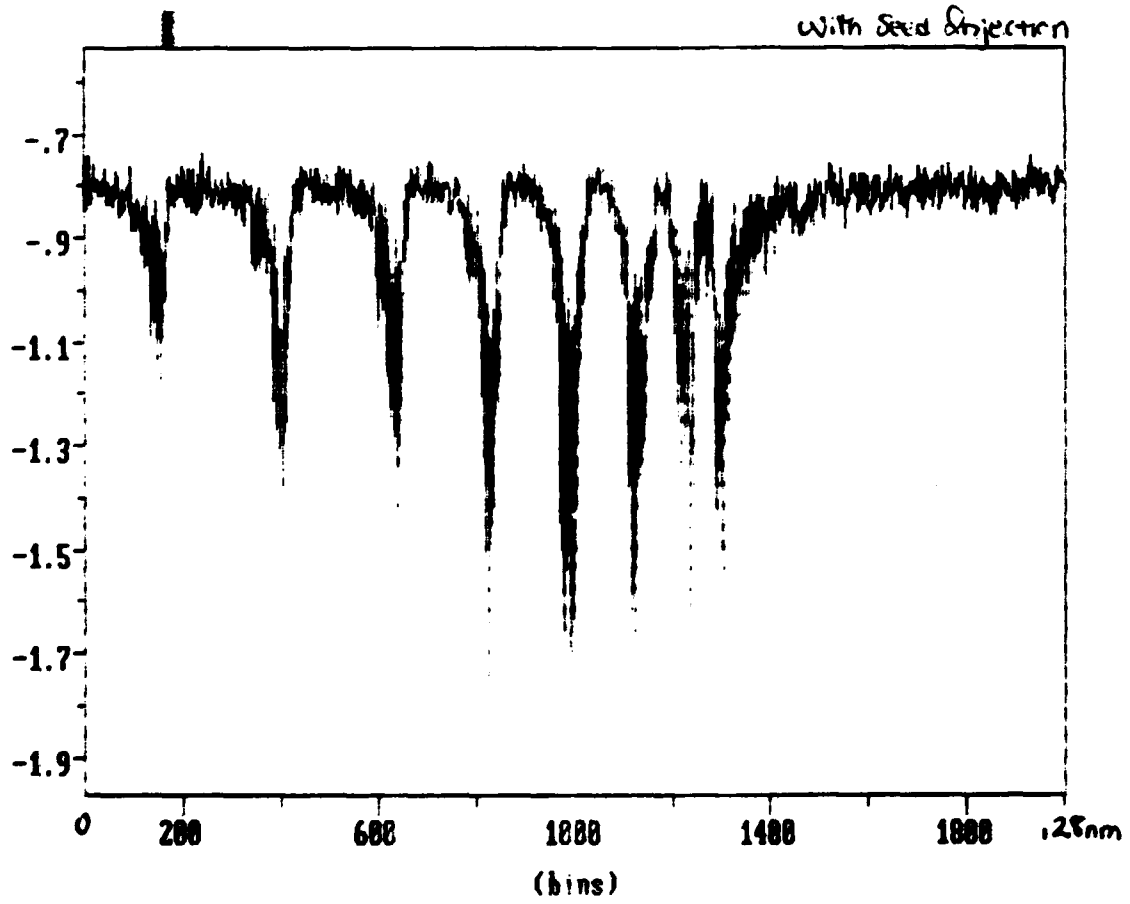
With Seed Injection
-.7
-.9
-1.1
-1.3
-1.5
-1.7
-1.9
0
200
600
1000
1400
1800
.28nm
(bins)

FIGURE 3

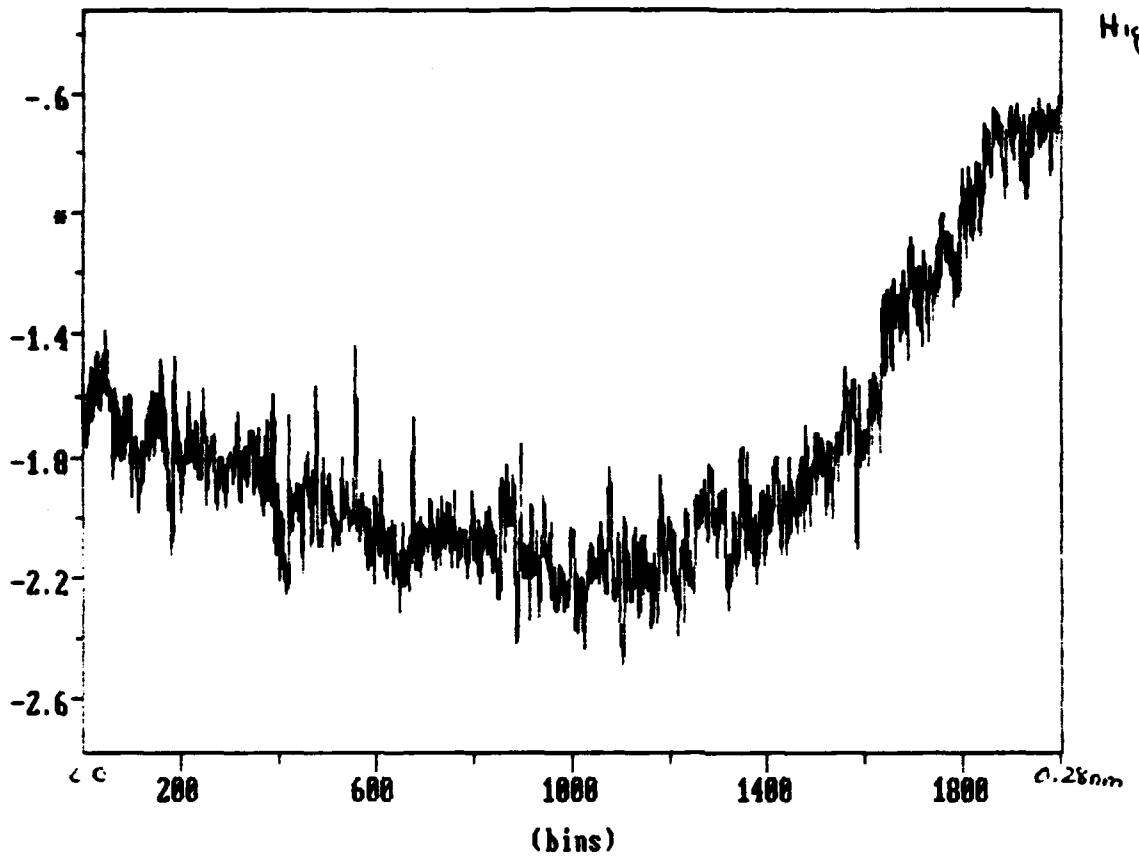
High Power
-.6
-1.4
-1.8
-2.2
-2.6
0.0
200
600
1000
1400
1800
0.28nm
(bins)

Figure 4

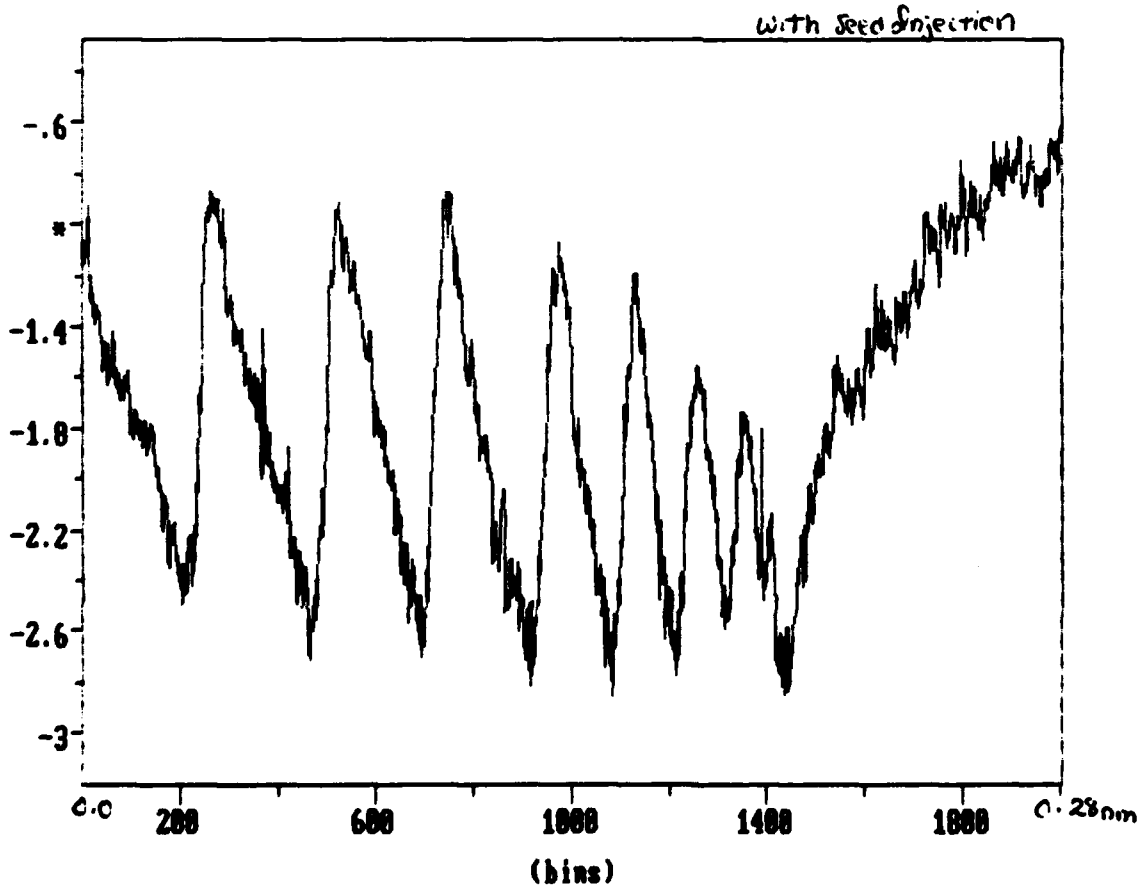
with seed injection
-.6
-1.4
-1.8
-2.2
-2.6
-3
0.0
200
600
1000
1400
1800
0.28nm
(bins)

VELOCITY MEASUREMENTS BY VIBRATIONAL TAGGING AND FLUORESCENT PROBING OF OXYGEN

by:

R. Miles
C. Cohen[a)]
J. Connors
P. Howard
S. Huang[b)]
E. Markovitz
G. Russell

Mechanical & Aerospace Engineering Department

PRINCETON UNIVERSITY
Princeton, New Jersey 08544

July 1987

ABSTRACT

We report here the development of a new method of "instantaneously" measuring three-dimensional velocity profiles and structure in air and oxygen. No seeding of particles, molecules, or atomic species is required. The method combines Raman Excitation plus Laser-Induced Electronic Fluorescence (RELIEF) to generate a time-gated image of the moving oxygen molecules.

The application of spectroscopy to the measurement of flow velocities and structure has contributed significantly to nonintrusive flow diagnostics. Numerous approaches have been studied, including fluorescence from atomic sodium in helium and nitrogen,[1,2] and fluorescence from molecular iodine in nitrogen and air.[3,4] These methods require seeding and have yielded time-averaged field measurements, but have not been capable of observing instantaneous three-dimensional profiles. Recently, Sell and Cattolica[5] have used a pulsed CO_2 laser to locally heat an ethylene seeded flow. They then followed the motion of the heated region by observing the photothermal deflection of a probe laser. This method gives an instantaneous velocity profile, but again, requires seeding. At NASA/Langley, stimulated Raman scattering in unseeded air is being used to measure flow velocity, temperature, and pressure.[6] This work is promising, but the signal is integrated along the laser path length, and the laser must be scanned in frequency. Consequently, the measurements are averaged over time and space.

The mechanism which we have developed for vibrationally tagging and following oxygen is Raman Excitation + Laser-Induced Electronic Fluorescence (RELIEF). Similar methods of optical double-resonant spectroscopy have been shown to be powerful tools for analyzing molecular structure. For example, the combination of stimulated Raman Excitation with Laser-Induced Fluorescence has been used to study the Raman spectrum of D_2CO.[7]

In our experiment, vibrational pumping by stimulated Raman excitation of oxygen is used to "tag" the flow. This is accomplished by two simultaneously pulsed high-power lasers whose frequencies differ by the vibrational frequency of oxygen (1555 cm^{-1}). These two lasers may be made colinear to mark a line, coplaner to mark a plane, or they may be made to intersect at single or multiple points depending upon the requirements of the experiment. The long lifetime of vibrationally excited oxygen (27 milliseconds in pure oxygen)[8] assures that these "tagged" molecules remain vibrationally excited while they move downstream. A short time after the oxygen has been tagged, it is interrogated with an argon-fluoride excimer laser, and the subsequent fluorescence is recorded with a high-sensitivity camera system. The measured displacement of tagged molecules gives a quantitative value of the flow velocities, and the observed structure of the tagged region gives a clear picture of the velocity profile.

The oxygen tagging was done using a Quantel Model YG592 Nd:YAG laser/dye laser system. The Nd:YAG laser was configured to give two frequency doubled .532μm beams, each with a pulse duration of approximately 10 nanoseconds. One beam had an energy of 400mJ per pulse and was used to drive the dye laser system. The other beam had an energy of 100mJ per pulse and was used for the stimulated Raman pumping. The dye laser was operated in the vicinity of .580μm and had an output energy of 40mJ per pulse. The dye and the frequency doubled Nd:YAG laser beams were combined so they propagated colinearly through the test cell. The frequency doubled Nd:YAG beam was delayed to optimize the time overlap. At the cell, the dye laser energy was 20mJ per pulse, and the doubled YAG was 50mJ per pulse.

The beams were focused into the cell with a 48 cm focal length lens. The tagging region was defined by the .532μm beam which was close to diffraction limited and had a diameter of 60μm between the e^{-2} intensity points at the center of the cell. The forward propagating Coherent Anti-Stokes Raman Scattering (CARS) was monitored to assure that the dye laser frequency was correct, and that the beams were optimally overlapped. The CARS spectrum of the Q branch of oxygen is shown in Fig. 1 for low and high power. The change in the line profile shows saturation and Stark broadening of the CARS process at high power, indicating strong vibrational pumping.

An energy level diagram of the excitation scheme is shown in Fig. 2. Stimulated Raman pumping occurs between the ground $^3\Sigma_g^-(v" = 0)$ and the first $^3\Sigma_g^-(v" = 1)$ vibrational states of the ground electronic manifold of oxygen. Interrogation is done with a Lambda Physik Model EMG 150MSC injection-locked argon-fluoride excimer laser which has a pulse duration of ~10 nanoseconds. This laser intersects the tagged region from above and further excites the $^3\Sigma_g^-(v" = 1)$ molecules to the $^3\Sigma_u^-(v' = 7)$ state of the Schumann-Runge Band. Fluorescence decay then occurs back to numerous vibrational states in the $^3\Sigma_g^-$ band. A diagram of the overlap of the argon-fluoride laser tuning range with the absorption lines of oxygen is shown in Fig. 3.[9] The argon-fluoride laser was tuned to the R[25] line. The linewidth of the argon-fluoride laser is 1 cm^{-1}, producing a good overlap with the 1.17 cm^{-1} linewidth of the transition.[10] The laser was focused with a cylindrical lens to form a 140μm thick by 1.23 cm wide sheet. The

measured energy passing through the tagged region was .019 joules, producing an energy fluence of 1.1 joules/cm^2, well above the .2 joules/cm^2 saturation fluence. The fluorescence yield is 10^{-5} due to the rapid predissociation rate of the Schumann-Runge bands.[10] The fluorescence spectrum was recorded through an optical fiber which collected light from the center of the test cell and transferred it to the spectrometer. The visible portion of that fluorescent spectrum is shown in Fig. 4. A General Electric Model TN2505 CID camera fitted with a gated double microchannel plate intensifier (ITT Model F4561) simultaneously imaged the fluorescence.

The timing in this experiment was done using a Stanford Research System Model DG535/5 delay generator which controlled the Q-switch opening time for the Nd:YAG laser, the firing time for the excimer laser, and the electronic gate for the camera intensifier. Timing accuracy is limited by laser jitter and is on the order of 2 nanoseconds. The minimum camera gatewidth was one microsecond, and the delay was set so that the camera was on during the argon-fluoride laser pulse.

A small oxygen jet was introduced into the test cell for demonstration purposes. Fig. 5 shows the fluorescence from the tagged line for interrogation delays of 0, 10, 20, 30, 40, and 50 microseconds. Each line on the figure represents a separate measurement. Calibration was accomplished by introducing a ruler into the test chamber at the tagging location and recording the image with the camera. These calibration lines are superimposed on the right side of the figure; the separation between lines is 1 mm. The data was taken by running the camera through a frame

grabber onto a videotape recorder and subsequently digitizing and repositioning the relevant frames.

In Fig. 5, the width of the lines and, consequently, the accuracy of the velocity measurement is limited by the resolution of the camera. The fundamental limit to the accuracy is determined by the actual width of the tagged lines and the elapsed time between tagging and interrogation. Molecular diffusion causes the width of the line to increase with time according to the relation

$$w = \sqrt{4\tau D + w_o^2}$$

where D is the molecular diffusion constant, τ is the time between tagging and interrogation, and w_o is the tagged line width at $\tau = 0$. A Gaussian profile has been assumed. For oxygen at room temperature and 1 atmosphere $D = .21\ cm^2/sec$. Using $w_o = 60\mu m$, the width of the line 50μ sec after tagging is $88\mu m$. Assuming the center of the line can be found to within 10% of the width, the accuracy of the measurement will be

$$\xi \approx \frac{.1w}{\Delta} = \frac{.1\sqrt{4\tau D + w_o^2}}{\tau v}$$

where Δ is the distance the tagged region has moved in time τ, and v is the flow velocity. At 50μ sec, the maximum Δ shown in Fig. 5 is $\sim$1.15 mm (v = 23 m/sec), so the accuracy limit is approximately .8%. Accuracy improves with increasing flow velocity and increasing time between tagging and interrogation.

Continuing work focuses on the application of this technique in well characterized jets as well as in high-speed turbulent flows under a variety of flow conditions and gas mixtures.

The authors would like to thank Prof. Will Happer and Dr. Jack Gelfand for their extremely helpful advice.

This work was supported by the Air Force Office of Scientific Research under Grants AFOSR-86-0191 and AFOSR-86-0219 (URIP).

FOOTNOTES

Present Addresses:

[a] RCA Astro Electronics
P.O. Box 800, M.S. 410-2-C17
Princeton, NJ 08543-0800

[b] Shanghai Changjiang Scientific
Instruments Factory
No. 45 Cao Xi Bei Road
Shanghai, P.R. China

REFERENCES

[1] M. Zimmermann and R.B. Miles, Appl. Phys. Letters 37, 885 (1986).

[2] S. Cheng, M. Zimmermann, and R.B. Miles, Appl. Phys. Letters 43, 143 (1983).

[3] J.C. McDaniel, B. Hiller, R.K. Hanson, Opt. Lett. 8, 51 (1983).

[4] M. Zimmermann, S. Cheng, and R.B. Miles, CLEO'82 Tech. Digest, Paper ThS4, Phoenix, Arizona, Opt. Soc. of America (1982).

[5] J.A. Sell and R.J. Cattolica, Appl. Optics 25, 1420 (1986).

[6] R.J. Exton and M.E. Hillard, Appl. Optics 25, 14 (1986).

[7] D.A. King, R. Haines, N.R. Isenor, and B.J. Orr, Optics Letters 8, 629 (1983).

[8] R. Frey, J. Lukasik, and J. Ducuing, Chem. Phys. Letters 14, 514 (1972).

[9] K. Yoshino, D.E. Freeman, and W.H. Perkinson, J. Phys. Chem. Ref. Data 13, 207 (1984).

[10] B.R. Lewis, L. Berzins, J.H. Carver, S.T. Gibson, J. Quant. Spectrosc. and Radiat. Transfer (GB) 36, 187 (1986).

FIGURE CAPTIONS

Fig. 1(a). CARS spectrum of oxygen (Q branch) at low power.

Fig. 1(b). CARS spectrum of oxygen (Q branch) at high power showing saturation broadening.

Fig. 2. Energy level diagram of the RELIEF scheme. Tagging is by stimulated Raman excitation of $^3\Sigma_g^-(v" = 1)$. Interrogation is by Laser-Induced Electronic Fluorescence for $^3\Sigma_u^-(v' = 7)$ following excitation with an ArF laser.

Fig. 3. Overlap of the ArF laser tuning curve with the transitions from the ground ($v" = 0$) and vibrationally excited ($v" = 1$) states of oxygen.

Fig. 4. Visible fluorescence spectrum following excitation of the R[25] line in the $^3\Sigma_g^-(v" = 4) \rightarrow {}^3\Sigma_u^-(v' = 7)$ band.

Fig. 5. Composite picture of tagged lines of oxygen across a small oxygen jet. The jet is located at the center of the line and is directed upward. Each line in the Figure corresponds to a separate experiment; they are offset for clarity. Interrogation is at 0, 10, 20, 30, 40, and 50 microseconds shown respectively from bottom to top. A millimeter scale is shown on the right side for quantitative velocity measurements.

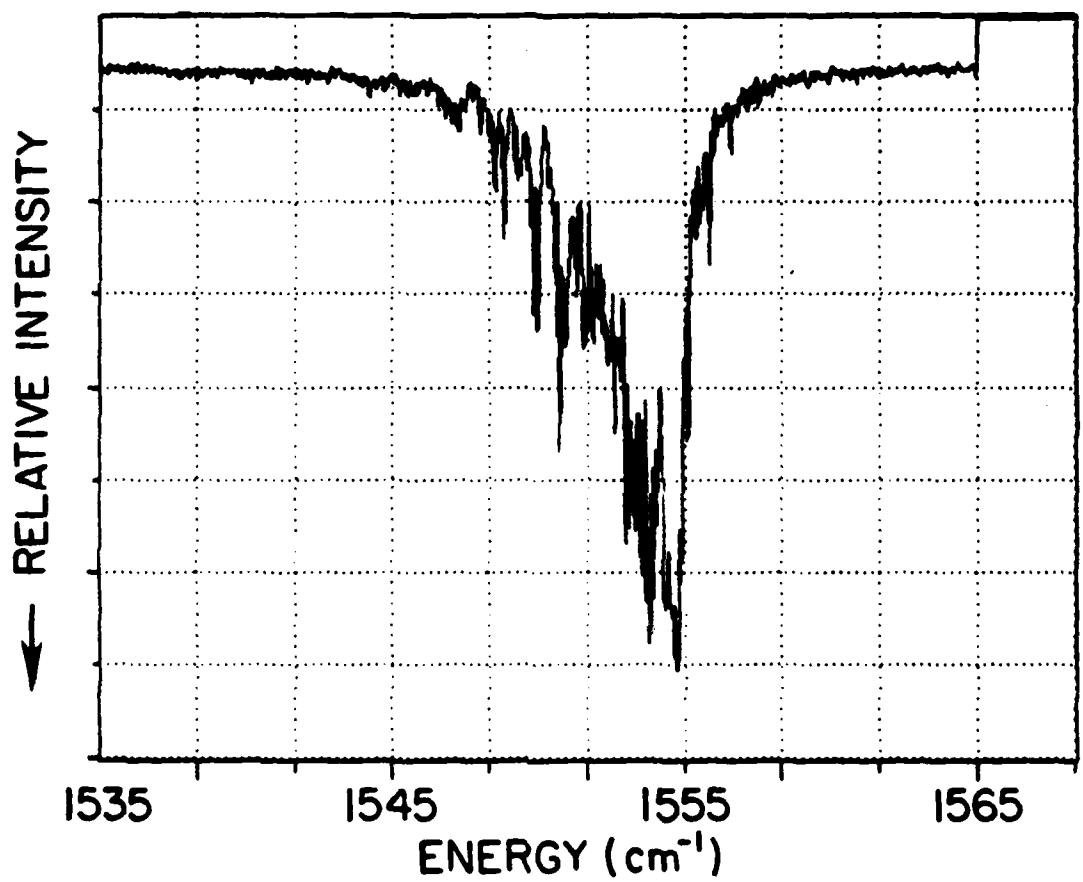

Fig. 1(a)

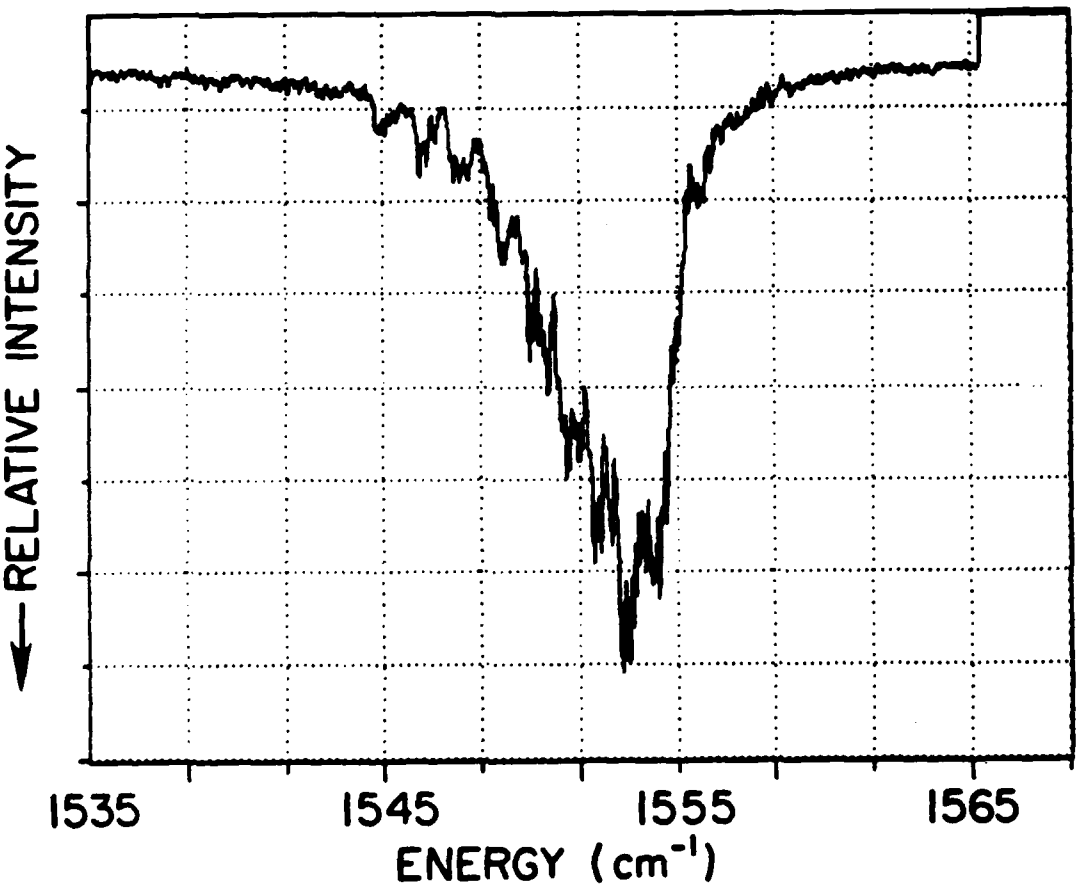

Fig. 1(b)

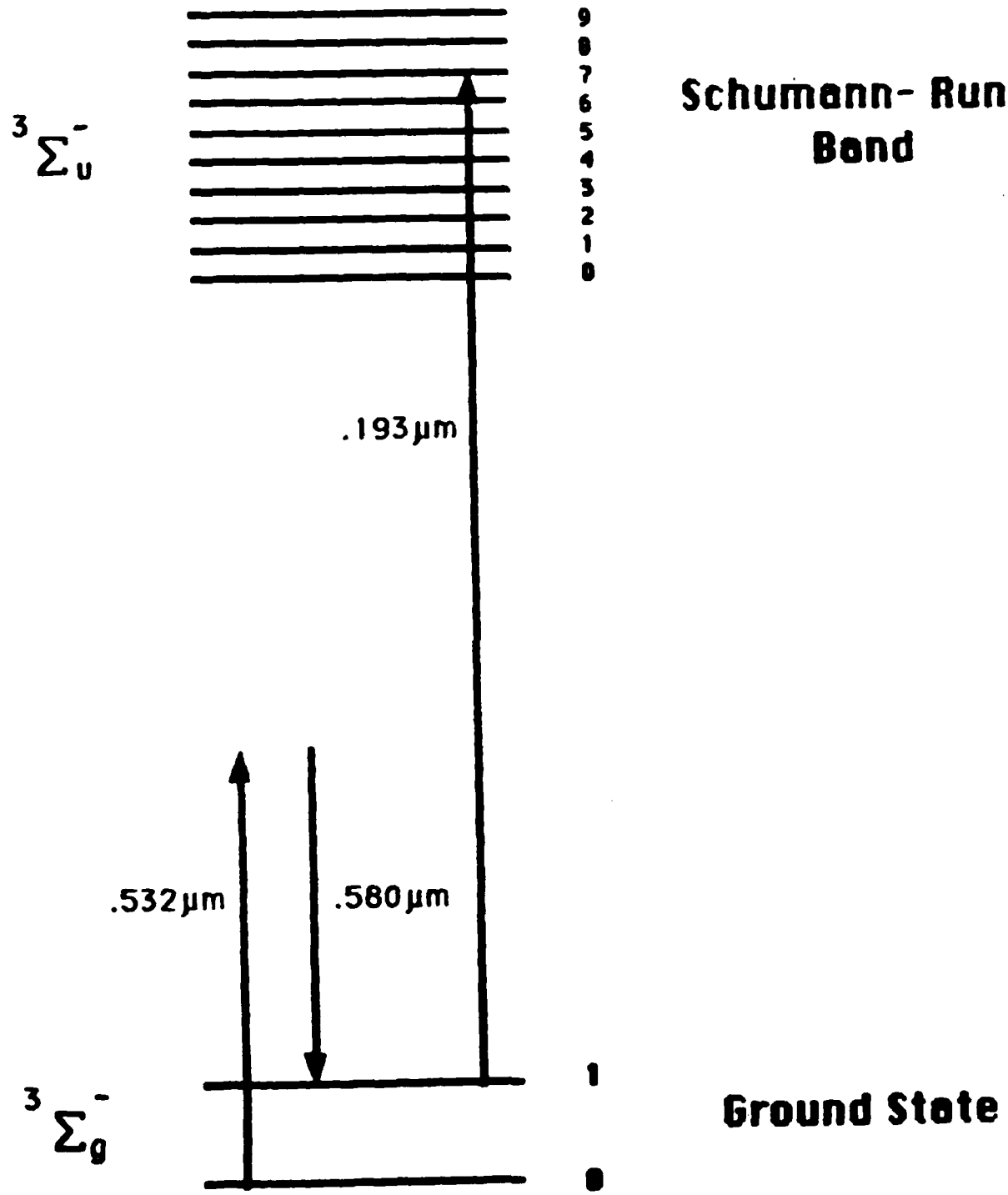

Fig. 2

(Revised 8/11/87)

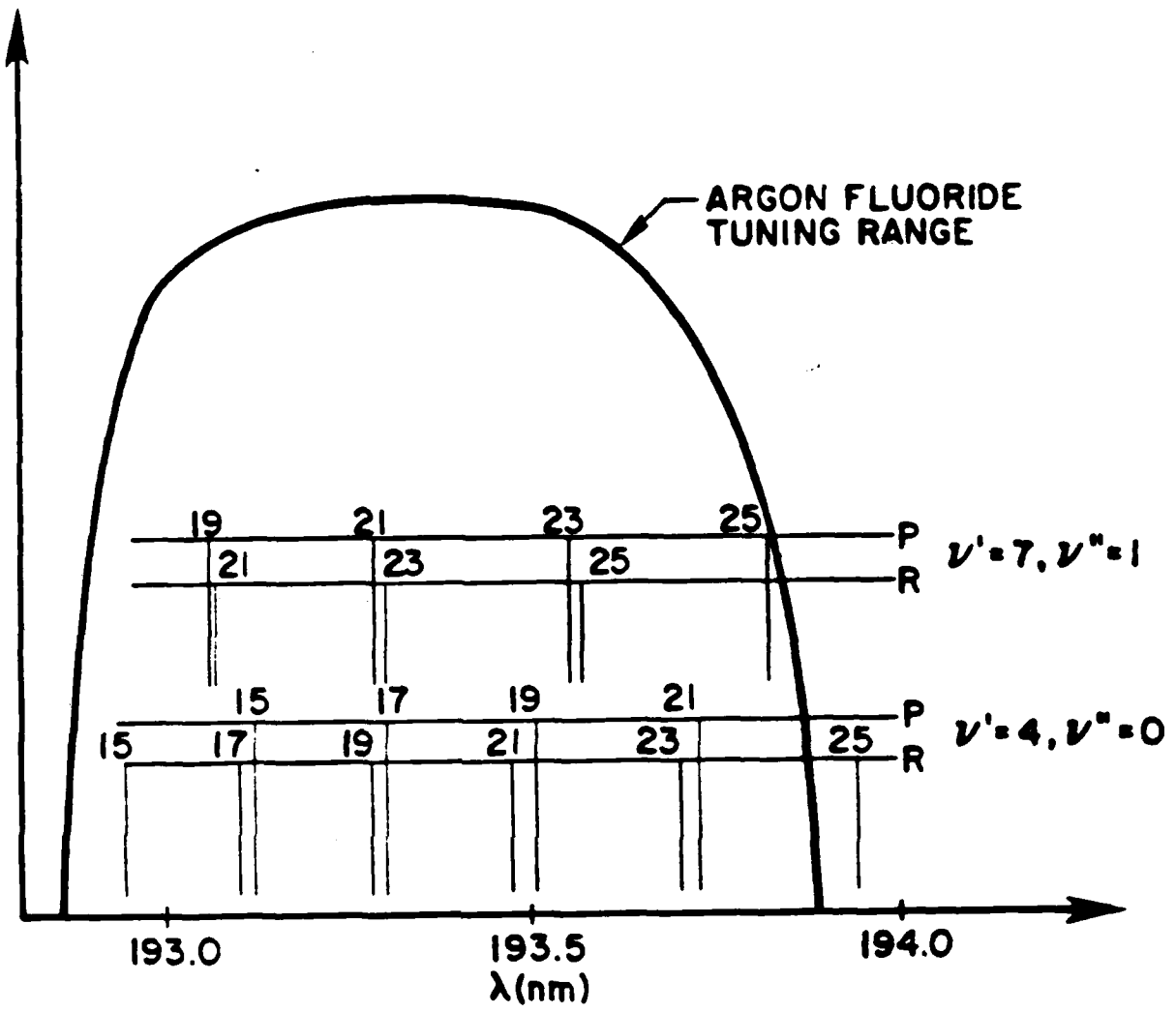

Fig. 3

(Revised 8/11/87)

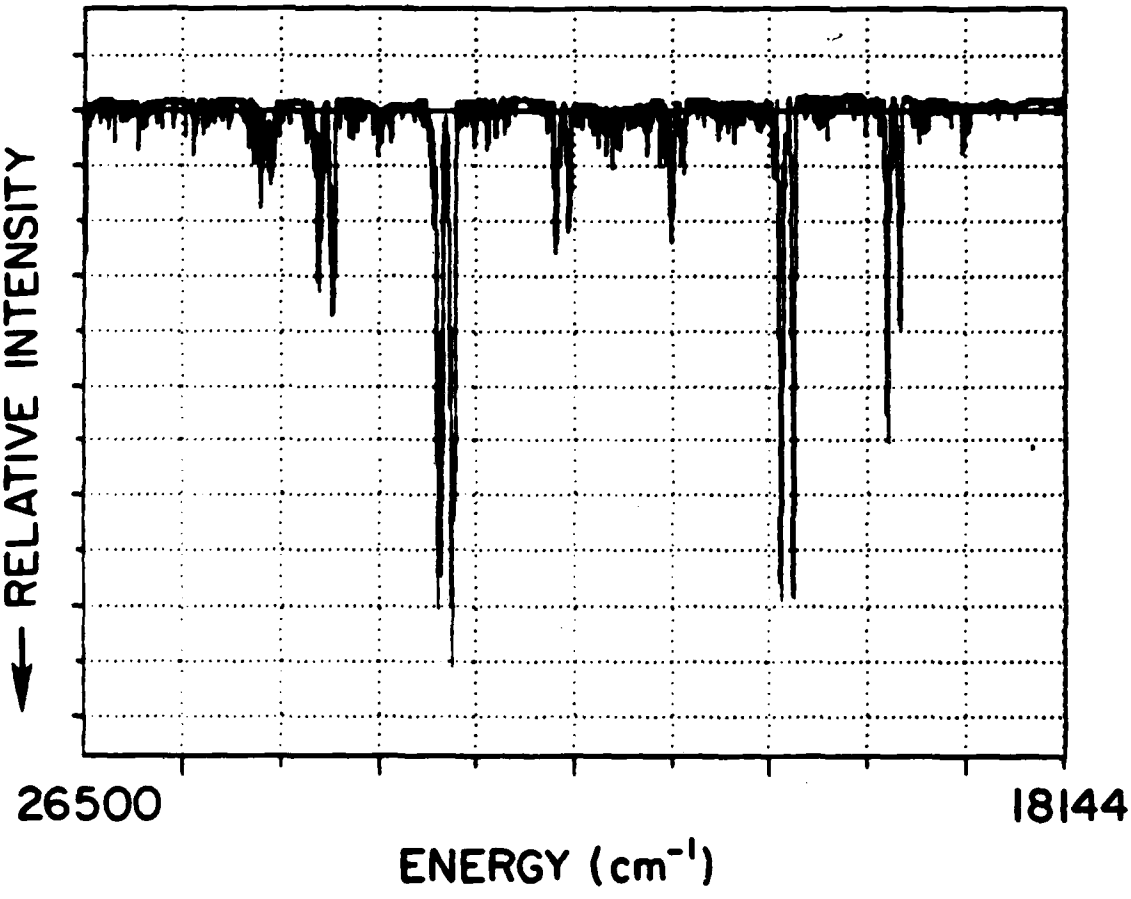

Fig. 4

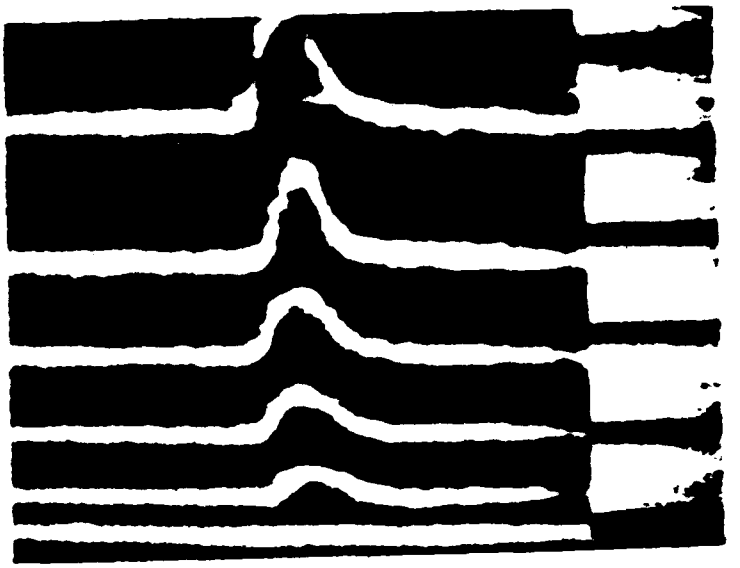

Fig. 5

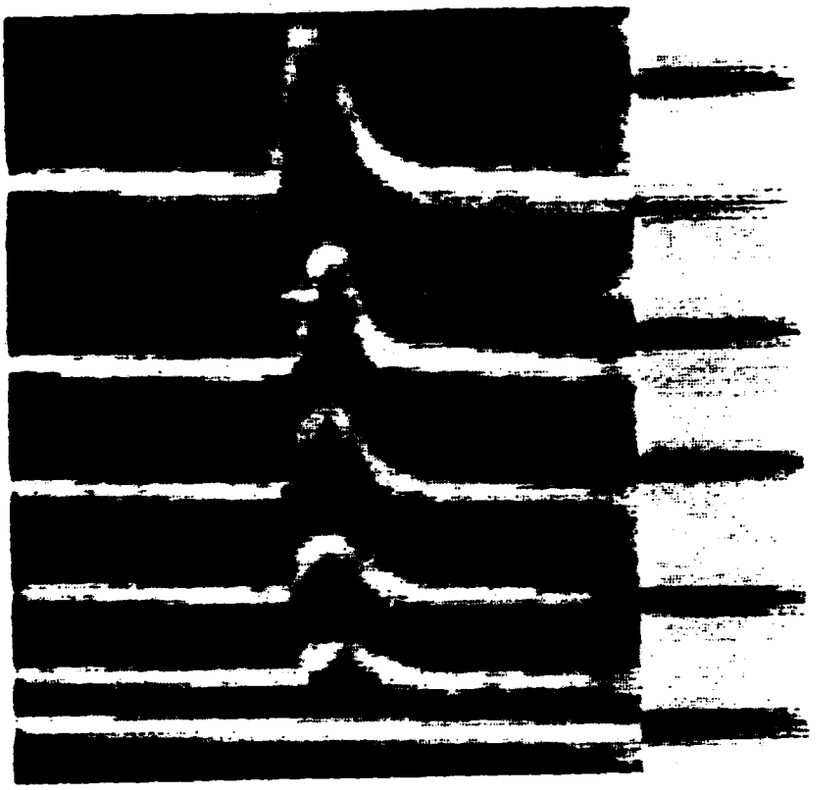

Fig. 5
(Half-tone)

Appendix E

SINGLE-PULSE TEMPERATURE AND DENSITY CROSS SECTIONS OF OXYGEN AND AIR

by:

Richard B. Miles
John J. Connors
Philip J. Howard
Edward C. Markovitz
Gregory J. Roth

Mechanical & Aerospace Engineering Department

PRINCETON UNIVERSITY
Princeton, New Jersey 08544

August 1987

ABSTRACT

A method for instantaneous two-dimensional measurements of temperature and pressure is presented. Laser-induced fluorescence following narrow line excitation of a specific oxygen resonance gives a direct measure of the population of a particular rotational vibrational ground state. Simultaneously, Rayleigh scattering from the same sample volume gives the total gas density. The ratio of these two measurements is directly related to the temperature.

We report here the development of a new method to simultaneously measure two-dimensional cross sections of temperature and density in air and oxygen with a single laser pulse. The method is similar to the temperature imaging method developed by Lee, Paul, and Hanson (1), but does not require constant pressure.

Massey and Lemon (2) originally proposed temperature measurements using one or two narrow linewidth argon-fluoride lasers to separately excite transitions from two different oxygen rotational states in sequential laser pulses. The fluorescence from these two states can be imaged and compared to determine the population ratio at each point, leading to a two-dimensional temperature and density measurement. This approach is limited by the noise associated with the low fluorescence yields of both signals and the fact that the first laser pulse heats the gas due to rapid predissociation of the oxygen, so the second laser pulse is not truly sampling an unperturbed flow region.

Our method uses a single pulse from an injection-locked, argon-fluoride laser. Light from the sample volume is simultaneously collected by two separate detectors or cameras. The first detector looks at the fluorescence following excitation of a particular rotation-vibration state as suggested by Massey and Lemon. The second detector observes the Rayleigh scattering at the laser wavelength. As will be shown, Rayleigh scattering is strong and depends predominately on density due to the large nonresonant contribution from the continuum of the Schumann-Runge band. Fluorescence, on the other hand, depends both on temperature and density.

By dividing the fluorescence signal by the Rayleigh signal, the temperature at any point can be uniquely determined. The low shot noise of the Rayleigh signal minimizes the noise caused by the division. If the mole fraction of oxygen is changing, the oxygen fluorescence can be ratioed to the oxygen Raman scattered light to eliminate the effects of gas mixtures but with a substantial increase in noise.

Rayleigh scattering has been used for two- and three-dimensional density measurements with substantial success (3). Work following the Massey and Lemon approach is underway at Stanford University (1,4), and two-dimensional imaging of oxygen in flames using laser-induced fluorescence has been done there and at Sandia Laboratories (5,6). Recently, laser-induced fluorescence from vibrationally tagged oxygen has been demonstrated as a method of velocity measurement (7).

Both Rayleigh scattering and laser-induced fluorescence can be derived from the polarizability of the molecule:

$$\alpha_{gi} = \frac{|\mu_{gi}|^2 \rho_g}{\hbar} \left[\frac{1}{\omega_{gi} - \omega - \frac{i\gamma_i}{2}} + \frac{1}{\omega_{gi} + \omega + \frac{i\gamma_i}{2}} \right] \qquad (1)$$

$$\alpha = \sum_{g,i} \alpha_{gi} \qquad (2)$$

where the subscript "g" refers to the ground states of the transitions and "i" refers to the upper states. μ_{gi} is the dipole moment, and ρ_g is the

population fraction of the ground state. The temperature dependence is contained in the f_g term:

$$\rho_g = \frac{(2J + 1)e^{-E(v,J)/kT}}{\sum_g \rho_g} \tag{3}$$

γ_i is the full width at half maximum of the resonance and depends predominantly on the lifetime of the upper state:

$$\gamma_i = A + D_i + Q_i \quad . \tag{4}$$

where A is the fluorescence rate, D_i is the predissocation rate, and Q_i is the quenching rate. For the oxygen Schumann-Runge band, $A = 5 \times 10^6$ sec^{-1} (2), compared to $D \tilde{=} 10^{-2}$ sec^{-1}. It is assumed that the quenching rate equals the gas kinetic collision rate, so separate collision broadening has been ignored.

Neglecting depolarization, the differential Rayleigh scattering cross section is:

$$\frac{\partial \sigma_R(\omega)}{\partial \Omega} = \frac{\omega^4}{(4\pi)^2 c^4 \varepsilon_o^2} \left| \alpha(\omega) \right|^2 \tag{5}$$

The total differential fluorescence scattering cross section is:

$$\frac{\partial \sigma_F(\omega)}{\partial \Omega} = \frac{1}{4\pi c \varepsilon_o} \sum_{gi} \left[\frac{A}{A + D_i + Q_i} \right] \omega_{gi} \, Im\left(\alpha_{gi}(\omega) \right) \tag{6}$$

The ratio $A/(A + D_1 + Q_1)$ represents a fluorescence efficiency or Stern Volmer factor.

We have constructed a computational model to evaluate the polarizability and the associated Rayleigh scattering and laser-induced fluorescence. This computational model has been compared to experiments to check its validity over a limited range. α_{gi}'s were computed using oscillator strengths from Huebner et al. (8) in the 7 to 14 eV range, and Ackermann et al. (9) and Krupenie (10) in the discreet regions of the Schumann-Runge band. Predissociation rates were taken from Lewis et al. (11).

The total oscillator strength for transitions below 14.09 eV is .383. As a consequence, additional nonresonant contributions to the polarizability must be expected from higher lying transitions. In order to account for these contributions, the polarizability was compared to measured values of the index of refraction in the 280 to 180 nm region (12). By including all transitions below 14.09 eV, the calculated index of refraction (n - 1) was found to be 41% of the measured index of refraction at STP. Since the additional contribution corresponds to transitions far from the area of interest, we corrected the polarizability by adding a constant and a frequency dependent factor:

$$\alpha = \alpha_{CALC} + \frac{2.710 \times 10^{-39}}{\lambda(nm)} + 1.254 \times 10^{-40} \qquad (7)$$

This produced results that were consistent with the experimental index of

refraction values throughout the visible and UV to within two percent. These added factors are not expected to change significantly with temperature in the regions of interest.

The computed fluorescence intensity as a function of laser wavelength and gas temperature was compared to measured values at 298 K, 396 K, 497 K, and 565 K. An injection-locked ArF laser intersected an atmospheric pressure, 7 mm diameter heated oxygen jet and was scanned in wavelength from 51646 cm^{-1} to 51772 cm^{-1}. The fluorescence was collected with a photomultiplier which was sensitive to only the visible portion of the spectrum. Simultaneously, a second photomultiplier monitored the Rayleigh scattering.

To compare with the measured values, the computed fluorescence was weighted to reflect that portion of the fluorescence spectrum falling in the visible (<30,000 cm^{-1}). Lines with low predissociation rates were found to have much less fluorescence than predicted unless a collisional quenching rate was included. A quenching rate of 1.0×10^{11} sec^{-1} gave the best fit to measurements. This fit was most sensitive to the 500 K and 565 K measurements since transitions to upper states with low predissociative rates can be seen at these temperatures.

Figure 1 shows the measured and computed fluorescence at 497 K as a function of laser wavelength. The computed spectrum has been convolved with a 1 cm^{-1} Lorentzian function to reflect the 1 cm^{-1} laser linewidth. Distortion of the spectrum has been minimized by careful purging of the

laser and laser beam path, and by dividing the fluorescence signal by the Rayleigh scattering.

Values of the fluorescence cross section and the Rayleigh scattering cross section were then computed across the tuning region of the argon-fluoride laser for temperatures ranging from 100 K to 1100 K. Figure 2 shows the visible portion of the fluorescence (<30,000 cm^{-1}), and the Rayleigh scattering as a function of laser frequency. The values of the Rayleigh cross section are absolute; the fluorescence intensities have been rescaled at each temperature so the structure can be seen. Note from these plots that the fluorescence signal is strongly temperature and frequency dependent, while the Rayleigh signal remains relatively constant ($\sim 5 \times 10^{-26}$ cm^2) and is, therefore, a good measure of density. The very *strong nonresonant* contributions to the polarizability dominate the Rayleigh scattering at low temperature, causing the temperature and wavelength dependent resonant contributions to be negligible. As the temperature increases, the resonant portion increases and its effects begin to become apparent. At very high temperatures (>1500 K), the resonant part dominates the nonresonant contribution and the structure of the Rayleigh scattering begins to echo that of the fluorescence.

By choosing a particular laser frequency and dividing the fluorescence signal by the Rayleigh scattered signal, a monotonic temperature variation can be observed. In Fig. 3, line a, the laser frequency is chosen at 51686.7 wavenumbers corresponding to the R(21) ($v'' = 0$ to $v' = 4$) transition to sample the ground vibrational state. In this case, the ratio

has good sensitivity to low temperatures. For higher temperatures, the argon-fluoride laser can be tuned to the R(25) (v" = 1 to v' = 7) transition at 51665.27 wavenumbers. The ratio of fluorescence to Rayleigh for that choice of laser frequency is shown in Fig. 3, line b. Here there is good temperature sensitivity above 400 K. Similarly, by selecting a laser wavelength to overlap a v" = 2 to v' = 10 transition, sensitivity to higher temperatures can be achieved.

Relatively good temperature sensitivity can also be achieved with a broad bandwidth argon-fluoride laser. The dispersive nature of the Rayleigh scattering resonances suggest that a broad bandwidth laser will see an even more temperature insensitive Rayleigh signal than a narrow bandwidth laser. Of course, the fluorescence yield will be significantly reduced, particularly at low temperature, where the laser overlap with the state-to-state transitions is limited. The ratio of fluorescence to Rayleigh scattering versus temperature integrated between 51590 cm^{-1} and 51893 cm^{-1} (the full linewdith of the ArF laser) is given in Fig. 3, line c. The fluorescence yield at low temperatures is very low, causing significant noise in the temperature measurement. The yield can be improved by a factor of 10 using a UV-sensitive camera and, more dramatically, by hydrogen Raman shifting the laser to the vicinity of 55850 cm^{-1} where strongly fluorescing v" = 0 to v' = 10 lines are accessible.

This work was supported jointly by the Air Force Office of Scientific Research and Lockheed-California Company.

REFERENCES

[1]M.P. Lee, P.H. Paul, and R.K. Hanson, Optics Ltrs. 12, 75 (1987).

[2]G.A. Massey and C.J. Lemon, IEEE J. Quant. Electronics QE-20, 454 (1984).

[3]B. Yip and M.B. Long, Optics Ltrs. 11, 64 (1986).

[4]M.P. Lee and R.K. Hanson, J. Quant. Spectrosc. Radiat. Transfer 36, 425 (1986).

[5]M.P. Lee, P.H. Paul, and R.K. Hanson, Optics Ltrs. 11, 7 (1986).

[6]J.E.M. Goldsmith and R.J.M. Anderson, Optics Ltrs. 11, 67 (1986).

[7]R. Miles, C. Cohen, J. Connors, P. Howard, S. Huang, E. Markovitz, and G. Russell, Optics Ltrs. (to be published 1987).

[8]R.H. Huebner, R.J. Celotta, S.R. Mielczarek, and C.E. Kuyatt, J. Chemical Physics, 63, 241 (1975).

[9]M. Ackerman, F. Biaume, and G. Kockarts, Plant. Space Sci. 18, 1639 (1970).

[10]P.H. Krupenie, J. Phys. Chem. Ref. Data 1, 423 (1972).

[11]B.R. Lewis, L. Berzins, J.H. Carver, and S.T. Gibson, Q.S.R.T. 36, 187 (1986).

[12]P.L. Smith, M.C.E. Huber, and W.H. Parkinson, Phys. Rev. A 13, 1422 (1976).

FIGURE CAPTIONS

Fig. 1. Measured and computed fluorescence at 497 K as a function of laser wavelength.

Fig. 2. Visible fluorescence and Rayleigh scattering as a function of laser wavelength for temperatures between 100 K and 1100 K.

Fig. 3. Ratio of visible fluorescence signal to Rayleigh scattering as a function of temperature. Lines a and b are with the laser tuned to transitions from the ground and first vibrational states, respectively. Line c is from a broad band laser source.

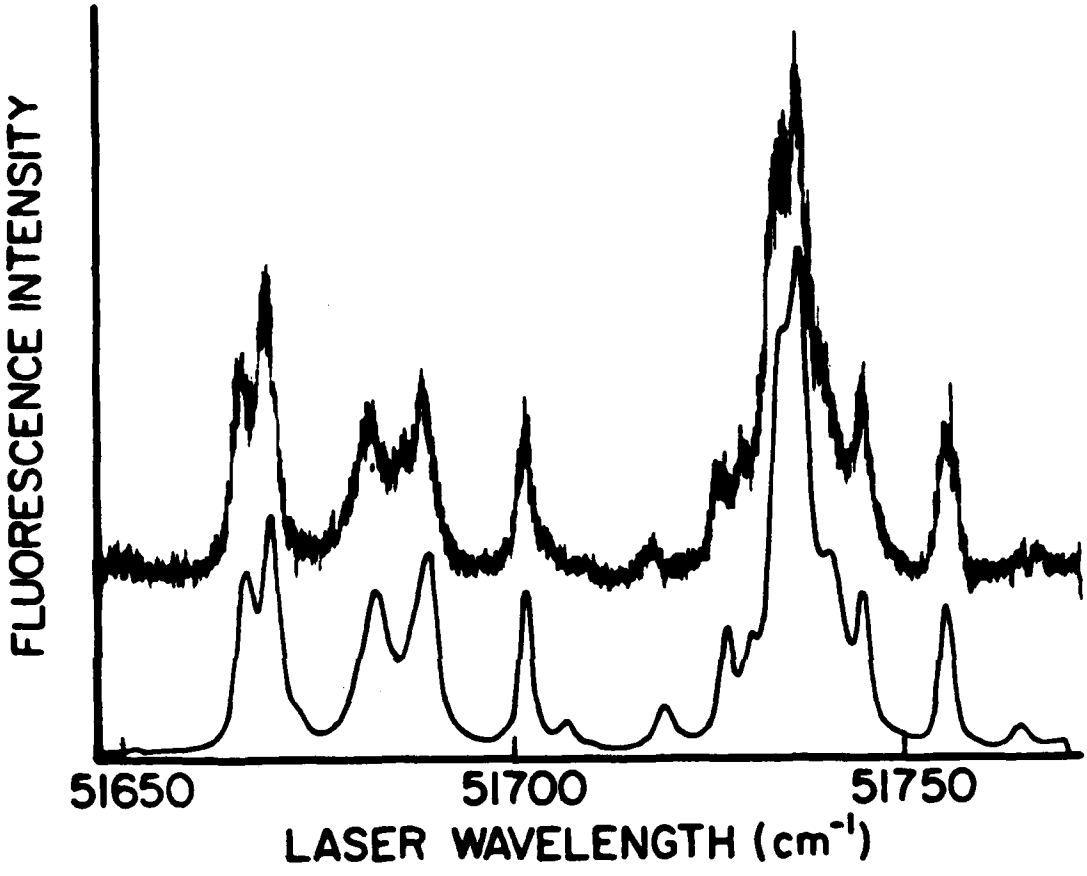
FLUORESCENCE INTENSITY
51650
51700
51750
LASER WAVELENGTH (cm⁻¹)

Figure 1

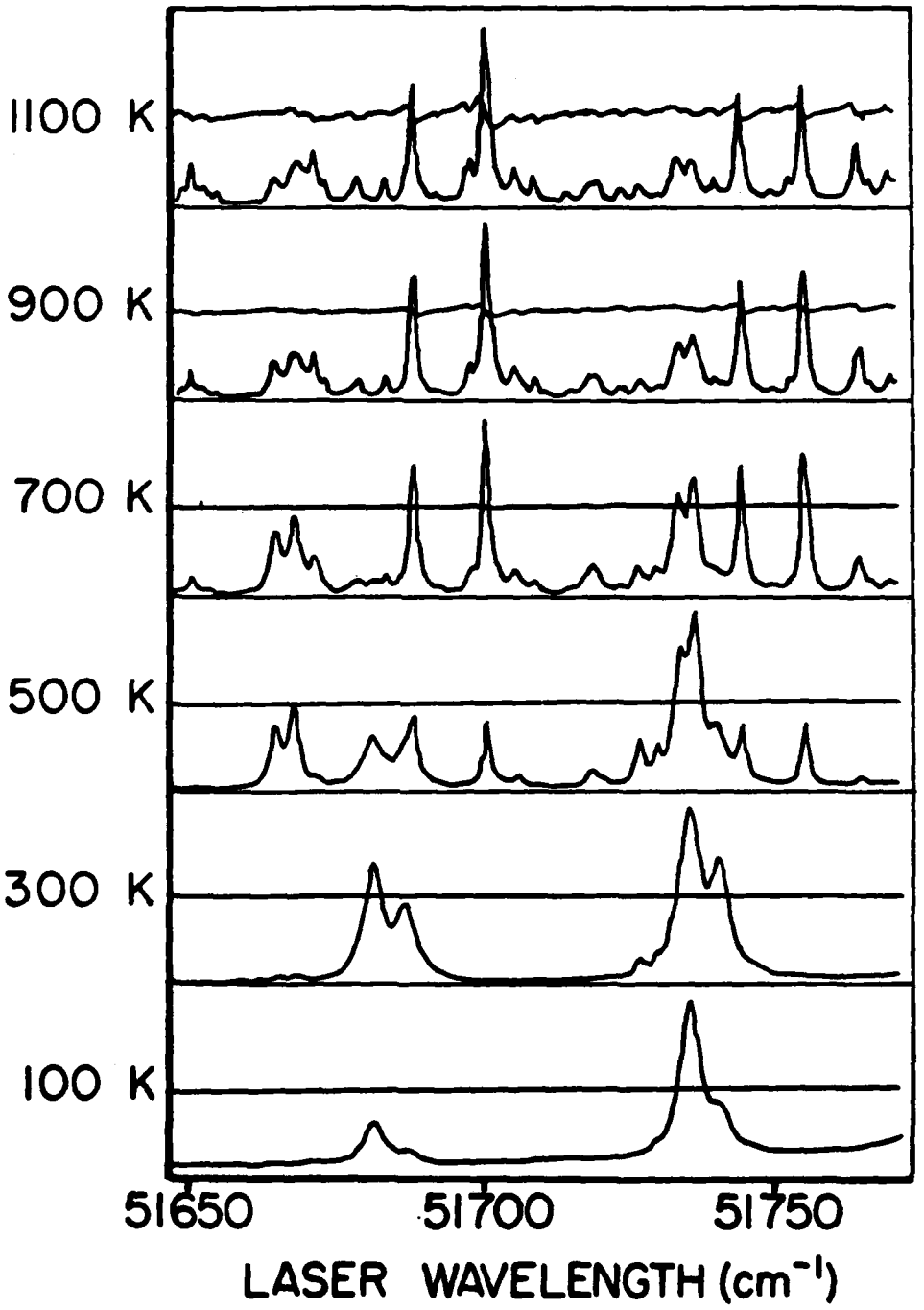
1100 K
900 K
700 K
500 K
300 K
100 K
51650
51700
51750
LASER WAVELENGTH (cm⁻¹)

Figure 2

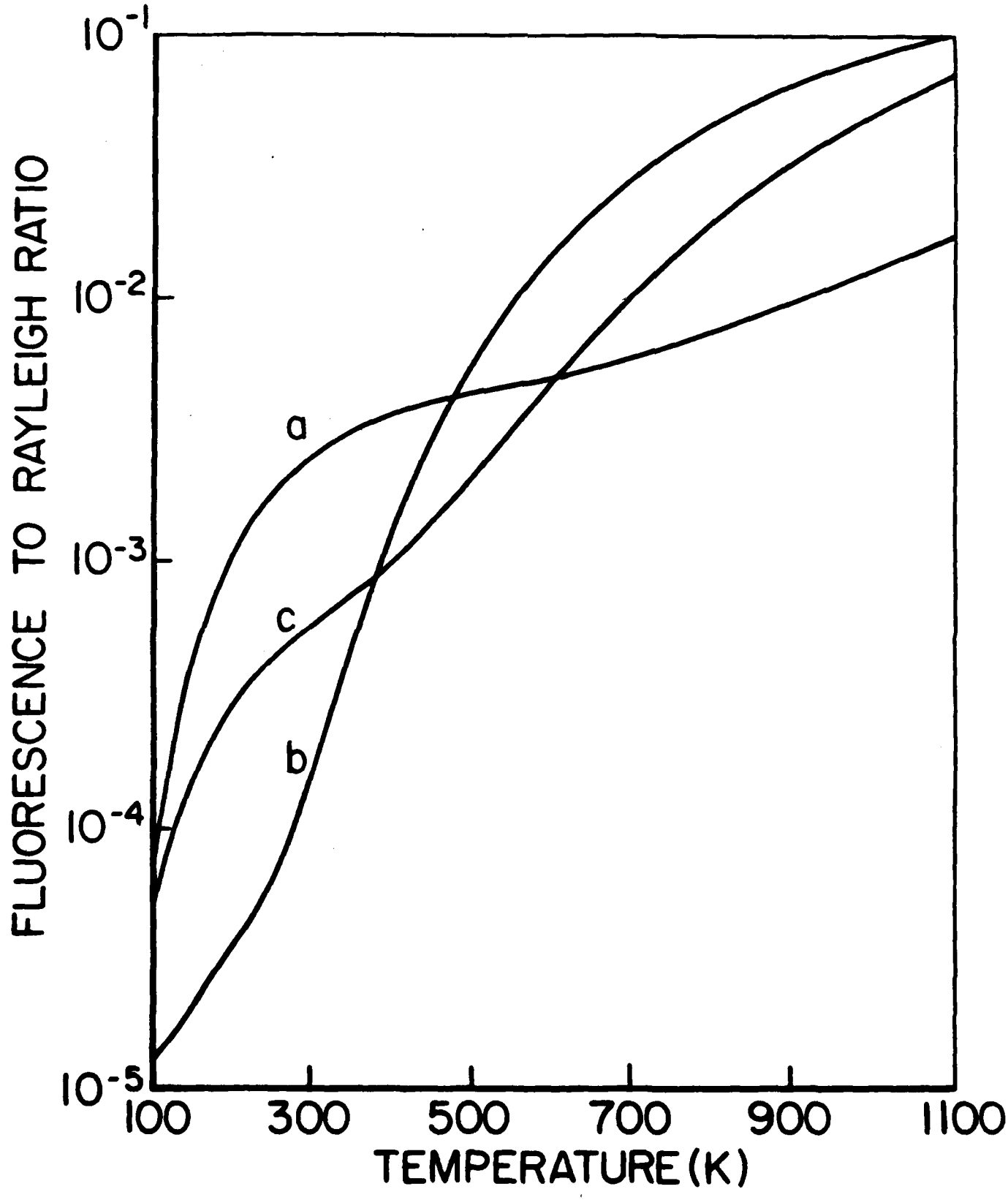
FLUORESCENCE TO RAYLEIGH RATIO
10-1
10-2
10-3
10-4
10-5
a
b
c
100
300
500
700
900
1100
TEMPERATURE (K)

Figure 3

END

FEB.

1988

DTIC